

## Evidence for Egg-Box-Compatible Interactions in Calcium–Alginate Gels from Fiber X-ray Diffraction

Pawel Sikorski,<sup>\*,†</sup> Frode Mo,<sup>‡</sup> Gudmund Skjåk-Bræk,<sup>‡</sup> and Bjørn T. Stokke<sup>†</sup>

Department of Physics and Norwegian Biopolymer Laboratory, Department of Biotechnology,  
Norwegian University of Science and Technology, Trondheim NO-7491, Norway

Received February 6, 2007; Revised Manuscript Received March 16, 2007

The structures of guluronic-acid-rich alginate in the acid and calcium forms were investigated using fiber X-ray diffraction. Data recorded for alginate fibers in the acid form show a repeat along the chain axis of  $c = 0.87$  nm, a value that is in agreement with the one measured by Atkins et al. (*Biopolymers* **1973**, *12*, 1865) and contradicts a repeat of 0.78 nm recently suggested by Li et al. (*Biomacromolecules* **2007**, *8*, 464). In the  $\text{Ca}^{2+}$  form, our observations indicate that the junction zone involves dimerization of polymer chains through  $\text{Ca}^{2+}$  coordination according to the egg-box model. For reasons that are not understood at present, coordination of the divalent cations reduces the ability for the lateral crystallographic packing of the dimers. A proposed model for the junction zone involves polymer chains packed on a hexagonal lattice with a lattice constant  $a = 0.66$  nm. Random pairs of chains form dimers through coordination of  $\text{Ca}^{2+}$  cations. Further lateral interaction between dimers is mediated by disordered  $\text{Na}^+$  and  $\text{Ca}^{2+}$  cations, water molecules, and hydrogen bonding.

### Introduction

For many ionic polysaccharides, the ability to bind divalent cations and form gels is the key to their biological functions as well as technological applications.<sup>1</sup> Alginic acid (alginate) is a copolymer of  $\beta$ -D-mannuronic acid (M) and  $\alpha$ -L-guluronic acid (G) (Figure 1). Alginate is a biopolymer mainly isolated from brown algae, and in recent years progress has been made in large scale bacterial synthesis of alginates with desired G and M composition as well as sequences.<sup>2–4</sup> Alginate belongs to a group of polymers used in the food and pharmaceutical industries as solution property modifiers and gelling agents. Alginates also have a recognized potential in the removal of toxic heavy metals from industrial wastes by biosorption.<sup>5</sup> Due to its industrial applications, the alginate gelation process has been studied extensively, but still some fundamental questions remain unresolved.

Numerous studies have been performed to characterize the mechanisms and structural features involved in the gelation of alginate. Gel formation is linked to specific and strong interactions between long stretches of G units and divalent cations such as  $\text{Ca}^{2+}$  or  $\text{Sr}^{2+}$ . The importance of the G units in this process is highlighted by the fact that the gel strength is directly related to the total content of G units and the average length of the G block in the gelling polymer.<sup>7</sup> Recent studies have also emphasized the importance of the MG repeating units.<sup>8</sup>

Morris et al.<sup>9</sup> have shown that  $\text{Ca}^{2+}$  cations induce interchain association and the formation of the gel junction zones. In the generally accepted model, referred to as the egg-box model,<sup>10</sup> divalent cations promote association of pairs of polymer chains (Figure 2a) and the formation of stable junction zones. The schematic egg-box association between G units, as proposed by Grant et al.,<sup>10</sup> is shown in Figure 2b. Two pairs of two consecutive G units, each pair belonging to different polymer

chains, are “glued” together through the coordination of a  $\text{Ca}^{2+}$  cation. The sugar ring of the guluronic acid is in the  ${}^1\text{C}_4$  conformation, and the polymer chain adopts a characteristic zigzag shape. It has been proposed that this shape creates pocket-like cavities in which  $\text{Ca}^{2+}$  cations can be easily accommodated. The dialysis experiment showed that a ratio of 4:1 between G units and  $\text{Ca}^{2+}$  cations exists in Ca–alginate gels.<sup>9</sup> This fits well with the egg-box model in which specific Ca-mediated interactions involve only two polymer chains (Figure 2), and in the gel state the junction zones do not show a long-range order. The egg-box model has also been used to describe the gelling of polygalacturonates (pectins),<sup>11–13</sup> but we restrict our investigation to the interaction between G-rich alginate chains.

To date, it has not been possible to verify the egg-box model for interchain association in alginate by any direct structural studies, for example, by fiber X-ray diffraction techniques. To our knowledge, no crystalline and well-resolved fiber X-ray diffraction patterns from  $\text{Ca}^{2+}$  or  $\text{Sr}^{2+}$  (or other divalent cations) forms of G-rich alginate have been published. The only available structural data is for the free acid form.<sup>14</sup> Some diffraction patterns of the low crystallinity  $\text{Ca}^{2+}$  form have also been published.<sup>15,16</sup>

The original egg-box model has been reconsidered on a few occasions in recent years. In none of the cases structural data for the  $\text{Ca}^{2+}$  form of alginate were used.<sup>12,15–19</sup> Braccini et al.<sup>12</sup> conducted molecular modeling studies in which the interaction between pure G-rich alginate polymer chains and  $\text{Ca}^{2+}$  cations were optimized. Using the geometry determined for the more crystalline acid form of the polymer chain, a model describing interchain association and  $\text{Ca}^{2+}$  binding was proposed. A different model was proposed by Arnott et al.<sup>17</sup> Using the original fiber X-ray diffraction data recorded for the acid form of the G-rich alginate,<sup>14</sup> the crystal structures of the acid and the  $\text{Ca}^{2+}$  forms were refined. Despite a lack of experimental data for the calcium form, a crystal structure and a  $\text{Ca}^{2+}$  coordination geometry were proposed. In the suggested structure,  $\text{Ca}^{2+}$  cations replace one of the water molecules found in the unit cell of the free acid form. The chain arrangement and the

\* Author to whom correspondence should be addressed. Phone: +4773598393. Fax: +4773597710. E-mail: pawel.sikorski@phys.ntnu.no.

<sup>†</sup> Department of Physics.

<sup>‡</sup> Norwegian Biopolymer Laboratory, Department of Biotechnology.

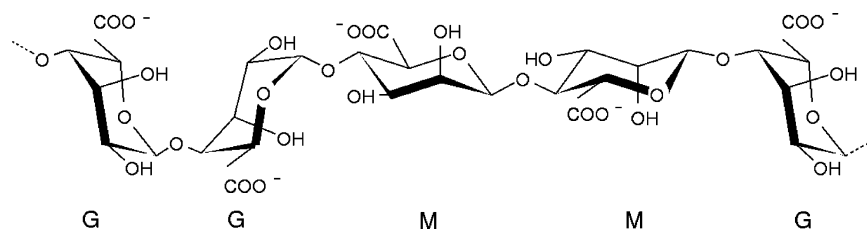


**Figure 1.** Structure of alginate.  $\beta$ -D-Mannuronic acid (M) and  $\alpha$ -L-guluronic acid (G). Ring conformations in the alginate chain (M:  ${}^4C_1$  and G:  ${}^1C_4$ ).<sup>6</sup>

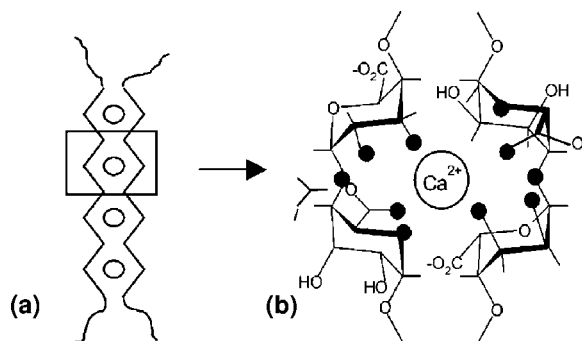


**Figure 2.** Schematic drawing and calcium coordination of the egg-box model as described for the pair of guluronate chains in calcium–alginate junction zones. Dark circles represent the oxygen atoms involved in the coordination of the calcium ion. Reprinted from ref 12. Copyright 2001 American Chemical Society.

position of the divalent cations are different from what has been proposed by Braccini et al.<sup>12</sup> and are also different from the original features of the egg-box model.<sup>10</sup>  $\text{Ca}^{2+}$  cations are involved in coordinating four polymer chains forming a well-organized network of Ca coordination and hydrogen bonding. This model suggests a long-range axial crystalline order within the junction zone.

Small-angle X-ray scattering (SAXS) measurements indicate that in the gel state the junction zone forms small crystallites incorporating a number of polymer chains. However, SAXS data does not provide any information regarding details of interchain interactions and chain packing but only describes the average size of the junction zones.<sup>18,19</sup> The SAXS data suggested that the dimerization of chain segments was the principal association mode at a low fractional  $\text{Ca}^{2+}$  saturation of guluronic acid in the alginate. An increase in the  $\text{Ca}^{2+}$  concentration resulted in increased lateral association.<sup>18,19</sup>

In their most recent contribution Li et al.<sup>16</sup> used fiber and powder X-ray diffraction patterns recorded from low crystallinity alginate samples to draw a number of conclusions about the structure of the junction zone of G-rich alginate in the acid and the  $\text{Ca}^{2+}$  forms. We will comment on the interpretation of the results and compare them with the data presented here.

## Experimental Section

Alginate from *Laminaria hyperborea* (stipe) with fraction of G units  $F_G = 0.67$ , fraction of two consecutive G units  $F_{GG} = 0.55$ , weight average molecular weight  $M_w = 400$  kDa, and an average length of G block longer than 1  $N_{G>1} = 14$  was used in all experiments. Fibers were prepared by extrusion of 1% Na–alginate solution into a gelling bath. Acidic (HCl, pH = 1) and low and high ionic strength calcium gelling baths (low, 100 mM  $\text{CaCl}_2$ ; high, 100 mM  $\text{CaCl}_2$  and 200 mM NaCl) were used. Fibers of lengths of up to 1 m could be prepared, and a typical gel fiber diameter was  $\sim 500$   $\mu\text{m}$  (Figure 3a). After gelation, the fibers were washed in a large amount of deionized  $\text{H}_2\text{O}$ .

**Table 1.** Comparison between Calculated and Observed  $d_{hkl}$ . Based on the Unit Cell  $a = 0.86$  nm,  $b = 1.07$  nm, and  $c = 0.87$  nm<sup>14 a</sup>

$hkl$	$d_{\text{cal}}$ (nm)	$d_{\text{obs}}$ (nm) $\pm 0.005$ nm	$I$ (abs)
110	0.670	0.665	s
020	0.535	0.530	w
200	0.430	0.427	m
111	0.531	0.527	w
002	0.437	0.432	m
012	0.403	0.400	s
102	0.388	0.388	s
112	0.365	0.365	m

<sup>a</sup> Here s represents strong, m represents medium, and w represents weak.

Some acid fibers were converted into the  $\text{Ca}^{2+}$  form by soaking in a  $\text{Ca}^{2+}$ -containing gelling bath. The gel fibers were then stretched using a TA-XT2 texture analyzer (Stable Micro Systems, Godalming, U. K.) as they dried slowly in air. The texture analyzer allowed stretching under controlled force–extension conditions. A typical stretch ratio obtained was  $\sim 100\%$ , and the typical drying/stretching time was 30 min. The final fiber diameter was 30–100  $\mu\text{m}$  (Figure 3b), and the final moisture content was below 5% (measured by determining the change in sample weight on drying in vacuum at 80  $^\circ\text{C}$  for 3 h).

X-ray diffraction patterns were recorded at the Swiss–Norwegian Beam Lines (SNBL), European Synchrotron Radiation Facility (ESRF), Grenoble, France ( $\lambda = 0.87$  Å, MAR345 detector) and also using a conventional generator with a Cu tube ( $\lambda = 1.54$  Å, patterns recorded using Fuji image plates (IPs) and read with Fuji IP reader). CCP13 software (<http://www.ccp13.ac.uk>) was used for background subtraction.

## Results and Discussion

A fiber X-ray diffraction pattern obtained from G-rich alginate in the acid form with good crystallinity and orientation is shown in Figure 3. Calculated and observed spacings of the main diffraction signals indexed using the unit cell parameters proposed by Atkins et al.<sup>14</sup> are listed in Table 1. There is good agreement between the observed and the calculated values, confirming that the unit cell is correct.

The diffraction data presented by Li et al.<sup>16</sup> have inferior resolution, which resulted in a number of misinterpretations. It was suggested that the repeat along the  $c$ -axis (chain axis) in the free acid form of G-rich alginate is close to 0.78 nm, compared to a value of 0.87 nm determined earlier.<sup>14</sup> For samples with poor crystallinity and orientation as those published by Li et al.,<sup>16</sup> the 002 reflection is very weak (compare patterns in Figure 3 with a lower crystallinity pattern shown in Figure 5a), and two strong signals at 0.403 and 0.388 nm (012 and 102) merge to form a strong broad signal located at around 0.39 nm. This is clearly visible in Figure 4, where diffraction data have been integrated and presented in the form of a powder diffraction pattern. The 0.39 nm signal was misindexed by Li et al.<sup>16</sup> as 002, where in fact in the powder diffraction pattern

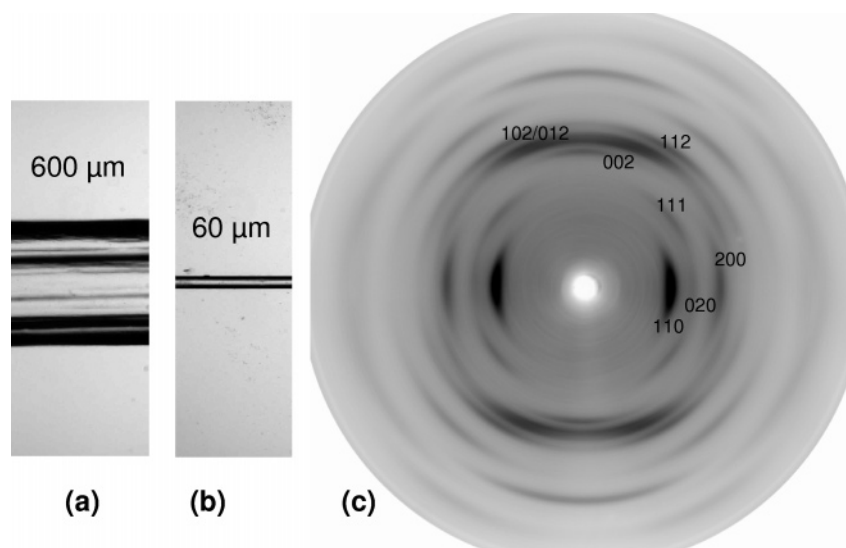


**Figure 3.** Optical micrographs of (a) gel and (b) dried–stretched alginate fibers. (c) Fiber X-ray diffraction pattern of G-rich alginate in the free acid form recorded at SNBL. Indices of the main diffraction signals are shown.

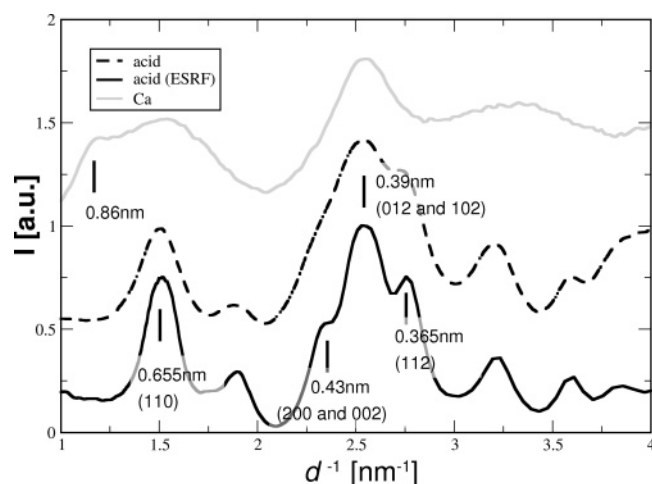


**Figure 4.** Fiber X-ray diffraction patterns for acid and  $\text{Ca}^{2+}$  forms of G-rich alginate that have been integrated and presented in the form of powder diffraction patterns. For the acid form, the 002 diffraction signal is not easily observed as it overlaps with the 200 signal.

the 002 signal is masked by the equatorial 200 signal (Figure 4). As the diffraction data presented here and data published by Li et al.<sup>16</sup> show the same main features we can argue that possible variations in the chemical composition of the alginate used in the two studies do not affect our conclusions (both polymers have similar total G-content).

More crucially Li et al.<sup>16</sup> used low-resolution diffraction data to suggest that in the  $\text{Ca}^{2+}$  form the G-rich alginate chain has a  $3_1$ -helical conformation. This is in contrast to the  $2_1$  conformation observed in the acid form. We do not agree with this interpretation of the diffraction results and present data that support a  $2_1$  conformation and the packing of the polymer chains within the junction zone compatible with the egg-box model.

Regardless of preparation and annealing procedures, we have not been able to prepare well diffracting crystalline samples of the  $\text{Ca}^{2+}$  form of G-rich alginate. It is possible to prepare samples with good orientational order of the polymer chains (i.e., nematic order), but the crystallinity is always low. The diffraction patterns observed for the  $\text{Ca}^{2+}$  form of G-rich alginate are very similar regardless of the sample preparation method. This includes gel fibers made by extruding alginate solution directly into a  $\text{Ca}^{2+}$ -containing solution (100 mM  $\text{CaCl}_2$ ), fibers

**Table 2.** Diffraction Signals Observed for  $\text{Ca}^{2+}$  Form of G-Rich Alginate<sup>a</sup>

$d_{\text{obs}}$ (nm) $\pm$ 0.01 nm		<i>I</i>
0.57	broad	s
0.86	sharp	m
0.39	broad	s

<sup>a</sup> Here s represents strong, m represents medium, and w represents weak.

converted from acid to the  $\text{Ca}^{2+}$  form, or the sample prepared by starting from a Na–alginate film that is then soaked in a  $\text{Ca}^{2+}$ -containing solution. It is known that the acid form is crystalline, and it is possible to convert it into the  $\text{Ca}^{2+}$  form by soaking in a  $\text{CaCl}_2$  solution (100 mM). Using this procedure, again only low crystallinity patterns similar to that shown in Figure 5b could be obtained. At the same time the orientation of the polymer chains within the sample was maintained (as indicated by the orientation order observed in the diffraction patterns). Surprisingly, on conversion back into the acid form (by soaking in a HCl solution, pH = 1), crystallinity was regained. These observations suggest that packing of the polymer chains in the  $\text{Ca}^{2+}$  form must be different from the acid form and there must be some inherent structural reason for the change in crystallinity.

A fiber X-ray diffraction pattern recorded for G-rich alginate in the  $\text{Ca}^{2+}$  form is shown in Figure 5b. Three main signals are observed: a broad and strong equatorial diffraction signal at 0.57 nm; a sharp, meridional or close to meridional signal at 0.86 nm; and a strong meridional or off-meridional signal at 0.39 nm (Table 2).

The meridional signal at 0.86 nm is especially interesting. The observed spacing is close to that predicted for the 001 reflection of the acid form ( $d_{001} = 0.87$  nm). However, in the acid form this reflection is systematically absent due to the  $2_1$  chain conformation. For a polymer chain in the  $2_1$  conformation, intensity close to the meridian on the first layer line is not expected even for a sample with poor crystallinity (see below). This signal is missing on a pattern recorded for stretched films of Na G-rich alginate (data not shown), a pattern which otherwise is similar to the one shown in Figure 5b.

We hypothesize that the distribution of  $\text{Ca}^{2+}$  cations within the junction zone contributes to the intensity observed close to the meridian on the first layer line. The distribution of strongly



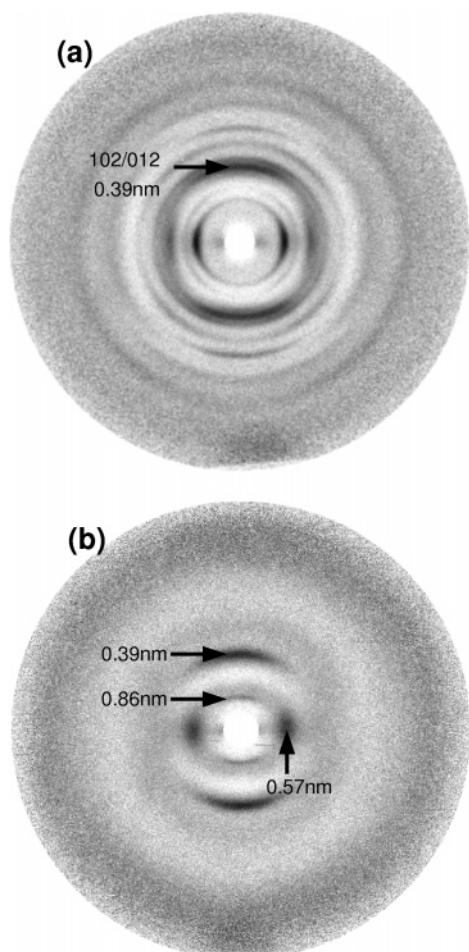


**Figure 5.** Fiber X-ray diffraction recorded for (a) the H<sup>+</sup> form gel fiber stretched by 100% and annealed for 24 h at 100 °C and high relative humidity and (b) the Ca<sup>2+</sup> gel fiber stretched 75% and annealed for 24 h at 100 °C and high relative humidity, prepared at high ionic strength conditions. Both patterns were recorded using a Cu tube X-ray source ( $\lambda = 1.54 \text{ \AA}$ ).

scattering Ca<sup>2+</sup> cations along the chain axis at a repeat distance of 0.86 nm would break the 2<sub>1</sub> symmetry. Interestingly, Ca<sup>2+</sup> cations separated by a distance of 0.87 nm along the chain axis are predicted by an egg-box-like interaction between alginate chains (four sugar units from two polymer chains coordinating a single Ca<sup>2+</sup> cation).

The intensity of the 001 diffraction signal is affected by the lateral order within the junction zone. Long-range order between dimers as shown schematically in Figure 6a would require Ca<sup>2+</sup> cations to be located at two defined crystallographic positions (axial translation with respect to each other by  $c/2 = 0.43 \text{ nm}$ ). This introduces additional symmetry to the structure (now also Ca<sup>2+</sup> cations follow the 2<sub>1</sub> symmetry), and the 001 signal should be systematically absent. Nonzero intensity of the 001 diffraction signal indicates that the association of dimers takes place through nonspecific interactions, such as water-mediated hydrogen bonding and disordered Ca<sup>2+</sup> and Na<sup>+</sup> cations (Figure 6b).

**3<sub>1</sub> versus 2<sub>1</sub> Conformation.** Before proposing a model for the junction zone, let us consider carefully the conformation of the alginate chain and investigate the diffraction pattern expected for a 3<sub>1</sub>-helical conformation as suggested by Li et al.<sup>16</sup> The diffraction from helical molecules has been studied extensively in the past.<sup>20–22</sup> A diffraction pattern for a single polymer chain in a helical conformation is described by the cylindrically average intensity transform of the discontinuous helix<sup>22</sup>

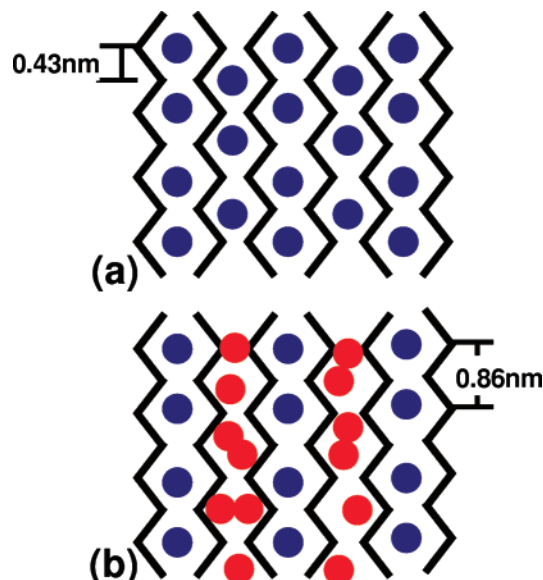


**Figure 6.** Schematic structure of G-rich alginate junction zone. (a) Long-range Ca<sup>2+</sup>-mediated interaction between chains. (b) Ca<sup>2+</sup>-mediated dimers that pack through unspecific interactions. The diffraction data points to the situation depicted in part b.

$$\langle I(R, l/c) \rangle_{\psi} = \sum_n J_n^2(2\pi Rr) \quad (1)$$

where  $l$  is the layer line index,  $c$  is the repeat along the chain axis,  $J_n$  denotes an  $n$ th order Bessel function,  $r$  is the helix radius, and  $R$  is the reciprocal space coordinate in the equatorial direction. The summation extends over all  $n$  values that satisfy eq 2

$$l = um + vn \quad (2)$$

where  $u$  is the number of units in  $v$  turns ( $u = 3$  and  $v = 1$  for a 3<sub>1</sub>-helix).

For a 3<sub>1</sub>-helix the diffraction pattern will contain layer lines spaced at  $c^{-1}$ . Diffracted intensities on the layer lines with  $l = 0, 3, 6, \dots$  are proportional to  $J_0^2 + J_3^2 + \dots$  and for  $l = 1, 2, 4, 5, 7, 8, \dots$  are proportional to  $J_1^2 + J_4^2 + \dots$ . Schematic diffraction patterns calculated for polymer chains in 2<sub>1</sub>, 3<sub>1</sub>, and 4<sub>1</sub> conformations using the CCP13 program HELIX<sup>23</sup> are shown in Figure 7. As expected from eq 1, intensity close to the meridian is observed only on the third, sixth, etc. layer lines for a 3<sub>1</sub>-helix, and it is zero on all other layer lines (Figure 7b). The described situation will not change significantly for a case where helices are arranged on a crystalline lattice. Instead of a continuous intensity, crystalline order will sample the intensity on the layer lines, and discrete spots will appear instead of continuous streaks. The intensity of the individual spots will still be proportional to what is seen for a single helix.

In the acid form, the G-rich alginate is in a 2<sub>1</sub> conformation, with a  $c$ -repeat of 0.87 nm. The advance per single G unit is 0.435 nm. If the chain was to be “twisted” into a 3<sub>1</sub> conformation, then the advance per monomer would most likely change by some small amount. Pectic acid, which is similar to guluronic acid, contains two equatorial linkages and exists in a 3<sub>1</sub> conformation.<sup>13</sup> For this polymer the axial advance per monomer is 0.445 nm.<sup>13</sup> In addition there is only a small change in the repeat distance between 3<sub>1</sub> and 2<sub>1</sub> conformations as shown by molecular modeling studies.<sup>12</sup> Therefore, we can assume that the advance per G unit for a hypothetical alginate chain in a 3<sub>1</sub> conformation would be between 0.40 and 0.45 nm. For a 3<sub>1</sub>

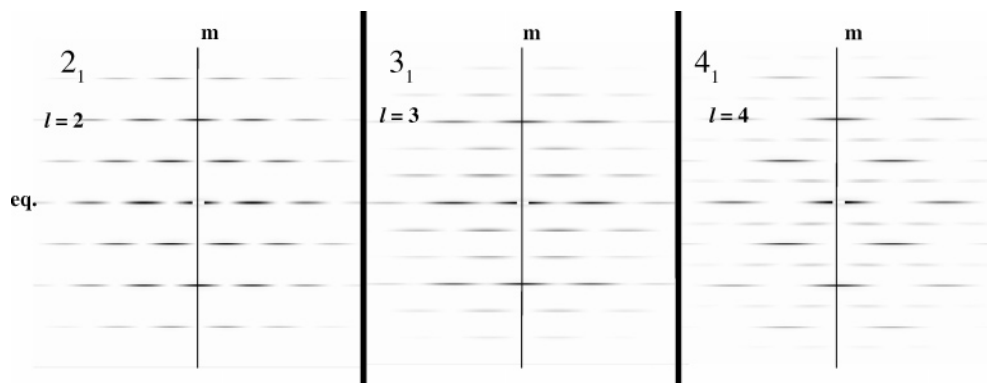


**Figure 7.** Schematic diffraction patterns calculated using the program HELIX<sup>23</sup> (<http://www.ccp13.ac.uk>) for polymer chains in a  $2_1$ -,  $3_1$ -, and  $4_1$ -helical conformations. Repeats along the  $c$ -axis are  $2c_0$ ,  $3c_0$ , and  $4c_0$ , where  $c_0$  is the rise per monomer unit. Note that meridional reflections are observed at the layer line with the same reciprocal coordinate corresponding to  $c_0^{-1}$ . Here eq represents equator, and m represents meridian.

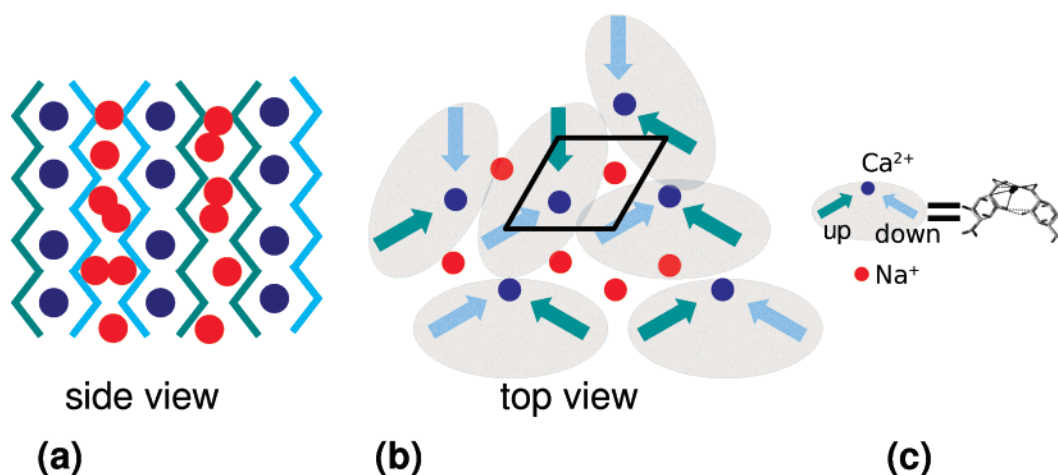


**Figure 8.** Hypothesized model for the chain packing within a G-rich alginate junction zone in agreement with the diffraction data. In part b alginate chains are represented by arrows, where green represents chain up and blue represents chain down; arrows are pointing toward  $\text{Ca}^{2+}$  cations (dark blue) coordinated by a given chain.  $\text{Na}^+$  cations are shown in red. There are only two chains per column of  $\text{Ca}^{2+}$  cations, and egg-box-like dimers are indicated by light gray ellipses. (c) Packing of chains in an egg-box-like dimer based on molecular simulations. A portion of part c was reproduced from ref 12. The average distance between polymer chains is 0.66 nm, but it is possible that this distance varies between  $\text{Ca}^{2+}$ - and  $\text{Na}^+$ -mediated interactions. This difference is however not resolved by the diffraction data, and the figure represents an average distance.

conformation, the repeat along the chain axis would contain three monomers, and as a consequence the  $c$ -repeat would be between 1.20 and 1.35 nm. Therefore, for a  $3_1$  conformation, layer lines at reciprocal coordinates  $(1.275 \pm .075 \text{ nm})^{-1}$ ,  $(0.638 \pm 0.038 \text{ nm})^{-1}$ , and  $(0.425 \pm 0.025 \text{ nm})^{-1}$  are expected. This is clearly not the case for patterns observed for the  $\text{Ca}^{2+}$  form of G-rich alginate presented here and those published by Li et al.<sup>16</sup> As a consequence, the  $3_1$  conformation for the  $\text{Ca}^{2+}$  form of the G-rich alginate can be ruled out.

As described above, the presence of meridional intensity on the first layer line (located at  $(0.86 \text{ nm})^{-1}$ ) cannot be interpreted as an indication of a  $3_1$ -helix but rather points to a chain in a  $2_1$  conformation with its symmetry broken by  $\text{Ca}^{2+}$  cations spaced by 0.86 nm.

**Chain Packing.** Data on the diffraction pattern allow us to construct a simple model for the  $\text{Ca}^{2+}$  alginate junction zone. We have to keep in mind that due to the low information content of the diffraction pattern this is not a definite model, but it represents one way to pack polymer chains that is consistent with the observed diffraction pattern.

Diffraction intensities observed on the first layer line are consistent with the basic scattering unit composed of two polymer chains in a  $2_1$  conformation coordinating one  $\text{Ca}^{2+}$  cation for every four G units (two in each chain). One way in which those dimers can then pack to form larger junction zones

is on a hexagonal lattice, as shown in Figure 8.<sup>24</sup> Figure 8b shows a view parallel to the polymer chain axis. Gray shaded ellipses represent two polymer chains that coordinate  $\text{Ca}^{2+}$  cations shown in blue (egg-box-like dimer). The polymer chains are centered on a hexagonal lattice. The lattice spacing can be calculated from the observed 0.57 nm diffraction signal, assuming that this is the first strong signal for a hexagonal lattice (100). The calculated lattice spacing that represents the average distance between the centers of the polymer chains is  $a = 0.66$  nm. This value is stereochemically feasible and similar to what has been found in molecular modeling simulations.<sup>12</sup>

## Conclusions

Fiber X-ray diffraction data recorded for G-rich alginate fibers in the acid form show a repeat along the chain axis of  $c = 0.87$  nm in agreement with the model by Atkins et al.<sup>14</sup> In the  $\text{Ca}^{2+}$  form, our observations indicate that the junction zone involves dimerization of polymer chains through  $\text{Ca}^{2+}$  coordination according to the egg-box model. For reasons that are not understood at present, coordination of the  $\text{Ca}^{2+}$  cations reduces the ability for lateral packing (smectic order) of the dimers. Hence, the reversible interconversion between acid and salt forms involves a shift in the balance between smectic (positional order) and nematic (only orientational order) order that is clearly

demonstrated by the fiber X-ray diffraction patterns. The proposed model for the junction zone involves a polymer chain packed on a hexagonal lattice with a lattice constant of  $a = 0.66$  nm. Random pairs of chains form dimers through the coordination of  $\text{Ca}^{2+}$  cations. Further lateral interaction between dimers is mediated by disordered  $\text{Na}^+$  and  $\text{Ca}^{2+}$  cations, water molecules, and hydrogen bonding.

**Acknowledgment.** P.S. acknowledges financial support from The Norwegian Research Council under Centre for Biopolymer Engineering at the Norwegian Biopolymer Laboratory, Norwegian University of Science and Technology (Grant No. 145945/130) and SNBL staff for help with the diffraction experiments (EXPERIMENT 01-02-649).

## References and Notes

- (1) Moe, S.; Draget, K. I.; Skjåk-Braek, G.; Smidsrød, O. In *Food Polysaccharides and Their Applications*; Stephen, A., Ed.; Marcel Dekker: New York, 1995; pp 245–286.
- (2) Valla, S.; Skjåk-Braek, G. *Agro-Food-Ind. Hi-Tech* **1996**, *7*, 38–41.
- (3) Rehm, B. H. A.; Valla, S. *Appl. Microbiol. Biotechnol.* **1997**, *48*, 281–288.
- (4) Ertesvag, H.; Valla, S. *Polym. Degrad. Stab.* **1998**, *59*, 85–91.
- (5) Davis, T. A.; Volesky, B.; Mucci, A. *Water Res.* **2003**, *37*, 4311–4330.
- (6) Smidsrød, O.; Glover, R. M.; Whittington, S. *Carbohydr. Res.* **1973**, *27*, 107–118.
- (7) Draget, K. I.; Skjåk-Braek, G.; Smidsrød, O. *Int. J. Biol. Macromol.* **1997**, *21*, 47–55.
- (8) Donati, I.; Holtan, S.; Mørch, Y. A.; Borgogna, M.; Dentini, M.; Skjåk-Braek, G. *Biomacromolecules* **2005**, *6*, 1031–1040.
- (9) Morris, E. R.; Rees, D. A.; Thom, D.; Boyd, J. *Carbohydr. Res.* **1978**, *66*, 145–154.
- (10) Grant, G. T.; Morris, E. R.; Rees, D. A.; Smith, P. J. C.; Thom, D. *FEBS Lett.* **1973**, *32*, 195–198.
- (11) Ravanat, G.; Rinaudo, M. *Biopolymers* **1980**, *19*, 2209–2222.
- (12) Braccini, I.; Perez, S. *Biomacromolecules* **2001**, *2*, 1089–1096.
- (13) Walkinshaw, M. D.; Arnott, S. *J. Mol. Biol.* **1981**, *153*, 1055–1073.
- (14) Atkins, E.; Nieduszynski, I.; Mackie, W.; Parker, K.; Smolko, E. *Biopolymers* **1973**, *12*, 1865.
- (15) Mackie, W.; Perez, S.; Rizzo, R.; Taravel, F.; Vignon, M. *Int. J. Biol. Macromol.* **1983**, *5*, 329–341.
- (16) Li, L.; Fang, Y.; Vreeker, R.; Appelqvist, I.; Mendes, E. *Biomacromolecules* **2007**, *8*, 464–468.
- (17) Arnott, S.; Bian, W.; Chandrasekaran, R.; Manis, B. *Fibre Diff. Rev.* **2000**, *36*, 44.
- (18) Stokke, B. T.; Draget, K. I.; Yuguchi, Y.; Urakawa, H.; Kajiwar, K. *Macromol. Symp.* **1997**, *120*, 91–101.
- (19) Stokke, B. T.; Draget, K. I.; Smidsrød, O.; Yuguchi, Y.; Urakawa, H.; Kajiwar, K. *Macromolecules* **2000**, *33*, 1853–1863.
- (20) Cochran, W.; Crick, F. H. C.; Vand, V. *Acta Crystallogr.* **1952**, *5*, 581–586.
- (21) Franklin, R. E.; Klug, A. *Acta Crystallogr.* **1955**, *8*, 777–780.
- (22) Fraser, R. D. B.; MacRae, T. P. *Conformation in Fibrous Proteins and Related Synthetic Polypeptides*; Academic Press: New York, 1973.
- (23) Knupp, C.; Squire, J. M. *J. Appl. Crystallogr.* **2004**, *37*, 832–835.
- (24) By hexagonal arrangement we do not mean a true hexagonal symmetry in a crystallographic sense. We envisage polymer chains located in a hexagonal lattice,  $a = 0.66$  nm, with complexing ions (Ca and Na) between the chains. The chain direction, the setting angle (rotation about the chain axis), and the positions of each type of complexing ion do not follow the hexagonal symmetry.

BM0701503